Glycobiology vol. 20 no. 5 pp. 576–585, 2010
doi:10.1093/glycob/cwq007
Advance Access publication on January 24, 2010

Application of electrospray mass spectrometry to the structural determination of glycosylphosphatidylinositol membrane anchors

Isabelle R.E. Nett[2], Angela Mehlert, Douglas Lamont, and Michael A.J. Ferguson[1]

Division of Biological Chemistry and Drug Discovery, College of Life Sciences, University of Dundee, Dundee DD1 5EH, Scotland, UK

Received on November 28, 2009; revised on January 16, 2010; accepted on January 17, 2010

The addition of glycosylphosphatidylinositol (GPI) anchors to proteins is an important posttranslational modification in eukaryotic cells. The complete structural elucidation of GPI anchors is a complex process that requires relatively large amounts of starting material. In this paper, we assess the degree of structural information that can be obtained by applying electrospray mass spectrometry and tandem mass spectrometry to permethylated GPI glycans prepared from a well-characterized GPI-anchored glycoprotein, the variant surface glycoprotein from *Trypanosoma brucei*. All GPI glycans contain a non-N-acetylated glucosamine residue, and permethylation leads to the formation of a fixed positive charge on the glycans, in the form of a quaternary amine. The permethylated glycans were detected as $[M + Na]^{2+}$ ions, and tandem mass spectrometry of these ions produced substantial, albeit incomplete, structural information on the branching patterns and linkage types for various GPI glycoforms of the variant surface glycoprotein.

Keywords: glycosylphosphatidylinositol/GPI anchor/mass spectrometry/*Trypanosoma brucei*/variant surface glycoprotein

Introduction

Glycosylphosphatidylinositol (GPI) anchored proteins (GPI-APs) are ubiquitous among the eukaryotes and are of considerable biological interest, with functions in cell protection, cell signaling, cell–cell adhesion and host cell–pathogen interactions (Ferguson et al. 2008; Paulick and Bertozzi 2008). GPI anchors are preassembled in the endoplasmic reticulum (ER) and added to the C-termini of certain proteins in the ER in exchange for the C-terminal signal peptide via a transamidation reaction (Ferguson et al. 2008; Fujita and Kinoshita 2010). The GPI anchor may then be further processed via lipid remodeling and carbohydrate side-chain modifications, in a protein and cell type specific manner, as the GPI-AP transits the secretory pathway (Ferguson et al. 2008; Fujita and Kinoshita 2010). The final destination for most GPI-APs is the outer leaflet of the plasma membrane or the topologically equivalent luminal surface of secretory granule membranes.

To elucidate the complete structure of a GPI anchor is a lengthy undertaking that requires relatively large amounts of native protein and techniques including 2D nuclear magnetic resonance spectroscopy, mass spectrometry and gas chromatography-mass spectrometry (GC-MS)-based composition and methylation linkage analyses, for example (Fankhauser et al. 1993; Ferguson et al. 1988; Homans et al. 1988; Schneider et al. 1990). However, with one exception (from the highly divergent protist *Entamoeba*; Moody-Haupt et al. 2000), all GPI anchors determined thus far share the common core structure of: $NH_2CH_2CH_2PO_4$H-6Manα1-2Manα1-6Manα1-4GlcNα1-6D-*myo*-inositol-1-HPO_4-lipid (EtN-P-Man_3GlcN-PI), where the amine of the ethanolamine phosphate (EtN-P) group is the attachment point to the α-carboxyl group of the C-terminus of the protein (Ferguson et al. 2008). In this paper, we exploit the chemistry of GPI anchors by using (a) aqueous hydrogen fluoride (HF) dephosphorylation to liberate the GPI anchor glycan from the parent GPI-AP and (b) permethylation to convert the free amine of the single non-N-acetylated glucosamine residue to a quaternary amine carrying a fixed positive charge. The permethylated GPI glycans ionize well in positive ion electrospray mass spectrometry (ES-MS), thanks in part to this quaternary amine feature (Baldwyn 2005). We assess the scope and limitations of structural interpretation that can be obtained from collision-induced dissociation (CID) tandem mass spectrometry (ES-MS/MS) of permethylated GPI glycans, using a series of well-characterized structures derived from a variant surface glycoprotein (VSG) from the protozoan parasite *Trypanosoma brucei*.

Results

Preparation and profiling of sVSG121 GPI glycans

In order to test the usefulness of electrospray tandem mass spectrometry for comprehensive GPI glycan characterization,

[1]To whom correspondence should be addressed: Tel: +44-(0)1382-344219; e-mail: m.a.j.ferguson@dundee.ac.uk
[2]Current address: Wellcome Trust Centre for Stem Cell Research and Cambridge Systems Biology Centre, University of Cambridge, Tennis Court Road, Cambridge, CB2 1QR, UK

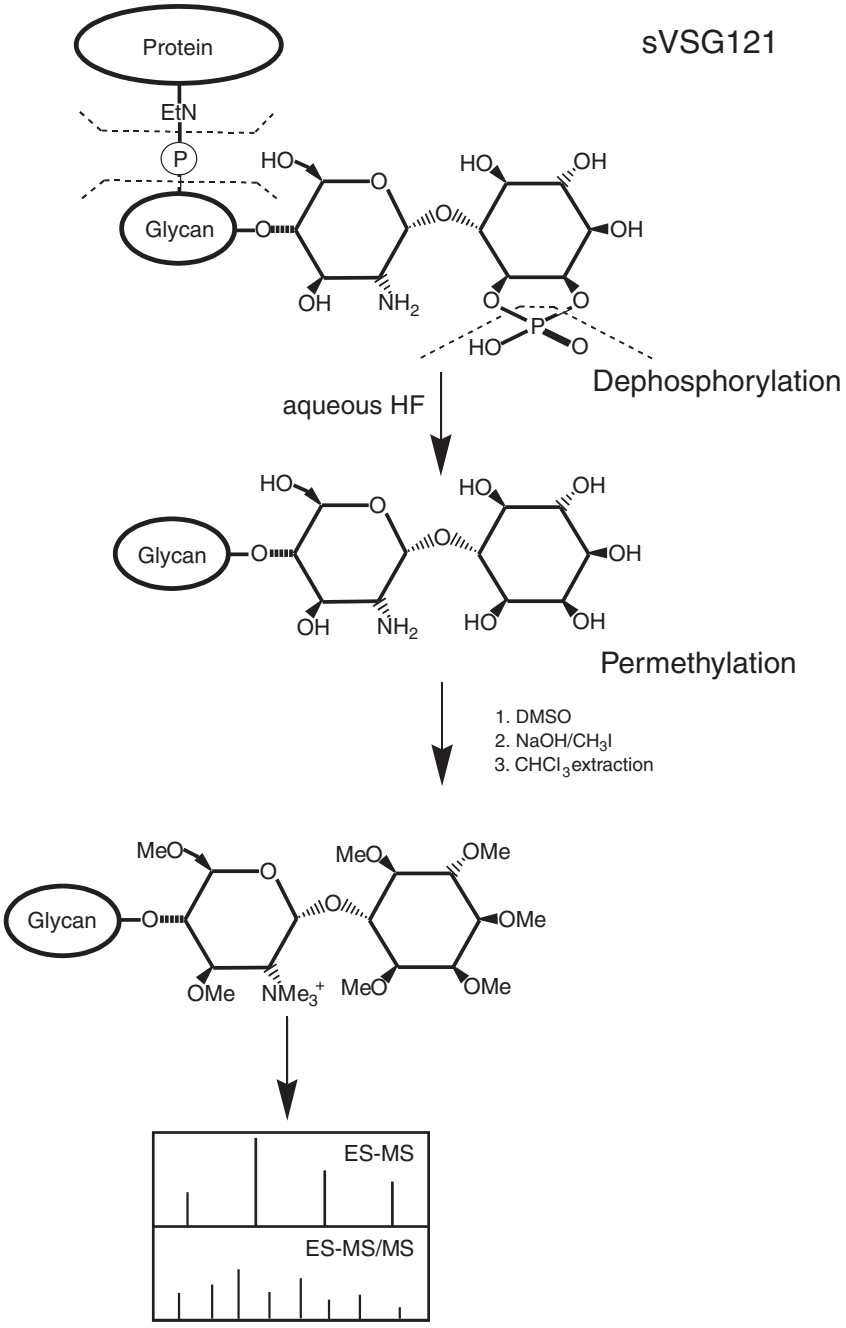

Fig. 1. General scheme for GPI structure determination using permethylation. The glycan fraction released by aqueous HF dephosphorylation was permethylated, recovered by solvent extraction and analyzed by ES-MS and ES-MS/MS.

the carbohydrate component of the sVSG121 GPI anchor was released from the GPI protein by aqueous HF treatment, permethylated and purified by solvent extraction (see Figure 1). The permethylated glycans were redissolved in 80% acetonitrile and 0.5 mM sodium acetate and analyzed by electrospray mass spectrometry, revealing three major isobaric forms of GPI glycan. The permethylated glycans contained a fixed positive charge due to the quaternary amine formed during methylation of the glucosamine residue and ionized as sodium adducts, producing doubly charged $[M + Na]^{2+}$ ions at *m/z* 871.9, 973.9 and 1075.9 (see Figure 2). These *m/z* values were consistent with fully permethylated glycan ions of composition $[Hex_6\text{-}HexN(Me_3)^+Ino + Na]^{2+}$, $[Hex_7\text{-}HexN(Me_3)^+Ino + Na]^{2+}$ and $[Hex_8\text{-}HexN(Me_3)^+Ino + Na]^{2+}$. Based on the known structure of the sVSG121 GPI anchor (Strang et al. 1993) and of the closely related sVSG117 and sVSG221 anchors (Ferguson et al. 1988; Mehlert et al. 1997), these ions can be further assigned to the compositions $[Gal_3Man_3GlcN(Me_3)^+ + Na]^2$, $[Gal_4Man_3GlcN(Me_3)^+ + Na]^{2+}$ and $[Gal_5Man_3GlcN(Me_3)^+ + Na]^{2+}$. The glycoform distribution shown in Figure 2 provides

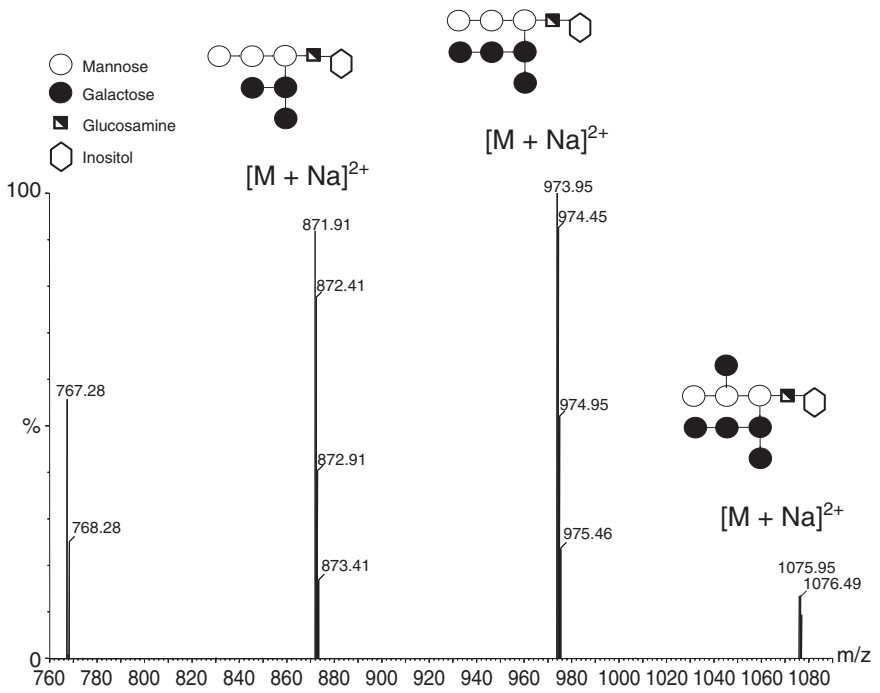

Fig. 2. ES-MS of permethylated GPI glycans of sVSG121. Ions at *m/z* 871.9, 973.9 and 1076.9 were consistent with $[M + Na]^{2+}$ ions of composition $[Hex_6\text{-}HexN(Me_3)^+Ino + Na]^{2+}$, $[Hex_7\text{-}HexN(Me_3)^+Ino + Na]^{2+}$ and $[Hex_8\text{-}HexN(Me_3)^+Ino + Na]^{2+}$, respectively.

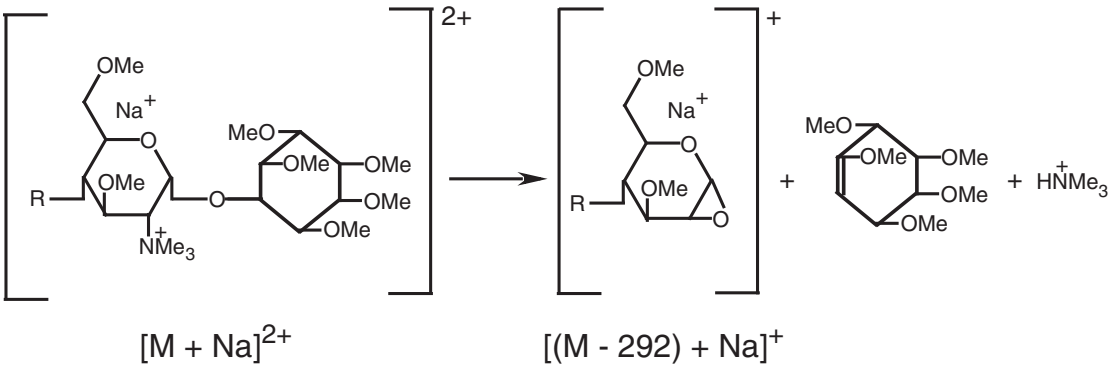

Fig. 3. Proposed fragmentation of permethylated GPI glycans that results in the simultaneous non-neutral loss of the permethylated D-*myo*-inositol moiety and quaternary ammonium group of the glucosamine.

a rough estimate of the relative amounts of the different species in the sample. Thus, according to the spectrum, the Gal_3- and Gal_4-glycoforms of sVSG121 were much more abundant than the Gal_5-glycoform, in agreement with the relative abundances observed by gel filtration of fluorescently labeled GPI glycans from the same glycoprotein (Zitzmann et al. 2000).

The doubly charged permethylated GPI glycoforms were selected for CID to provide structural information, in particular to define sequence, branching and linkage details. The precursor $[M + Na]^{2+}$ ions produced singly charged product ions arising predominantly from cleavage across the glycosidic bonds together with a number of additional product ions derived from cross-ring cleavages, as will be discussed later. The nomenclature used to define fragmentation is based on that introduced by Domon and Costello (1988). In this instance, an α suffix is used to designate cleavages in the GPI anchor mannosyl core and a β suffix for cleavages in the 3-linked alpha-galactose branch attached to the GPI core. Fragments derived from cross-ring cleavages are A-type ions, where the superscript defines the position of the cleavage after the corresponding carbon atom of the sugar ring.

Sequence, branching and linkage assignments for the Gal_3 GPI glycan glycoforms

Fragmentation of the doubly charged precursor ion at *m/z* 871.9 produced singly charged product ions, which were observed as an $[M + Na]^+$ ion series. The most abundant

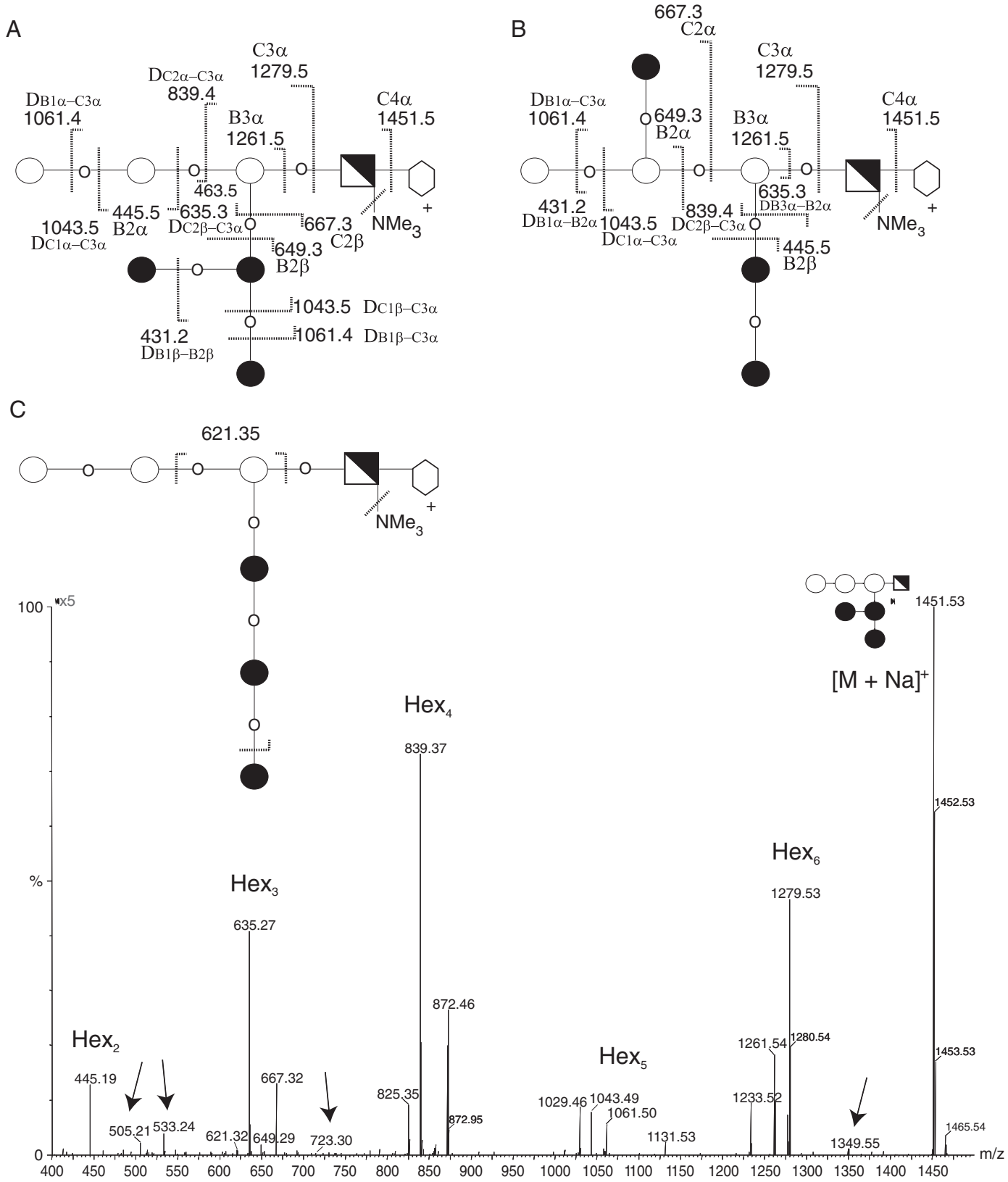

Fig. 4. Product ion spectrum of the permethylated Gal_3 glycoform of the $[M + Na]^{2+}$ precursor ion (*m/z* 871.9). For further discussion, see text.

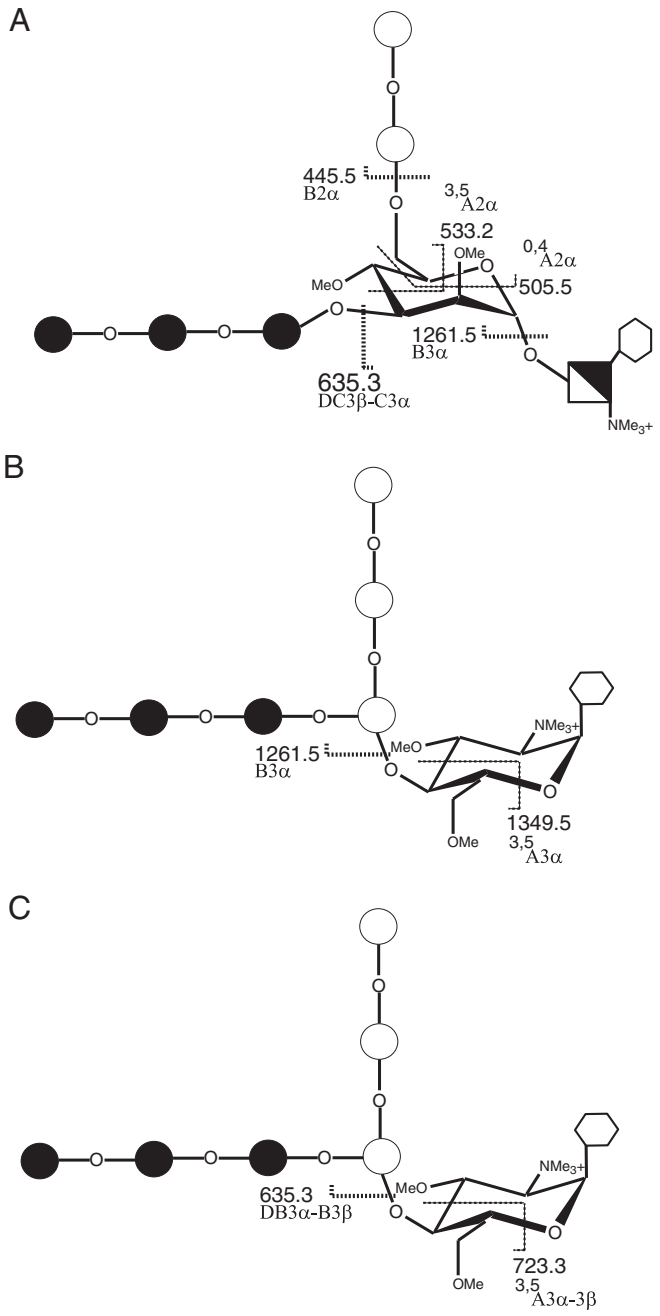

Fig. 5. Cross-ring fragmentation of the permethylated GPI Gal_3-glycoform of the doubly charged precursor ion at *m/z* 871.9. The A-type ions observed are shown in Fig. 3. For further discussion, see text.

product ion was *m/z* 1451.5, which corresponded to the permethylated glycan lacking the D-*myo*-inositol and quaternary ammonium group of the glucosamine. This non-neutral loss (see Figure 3) dominates the MS/MS spectrum since almost all of the other ions are the products of *m/z* 1451.5 (Figure 4). A pair of the product ions was observed at *m/z* 1279.5 and 1261.5 resulting from C- and B-type cleavage at the Manα1-4GlcN glycosidic bond, and further glycosidic bond cleavages within these metastable ions produced a number of double-cleavage ions, as indicated in Figure 4.

The presence of double glycosidic cleavage fragments, termed D-ions, could be used to define the branching topology (a detailed overview of how to analyze interresidue linkages and branching patterns of permethylated glycans by CID is given in Reinhold et al. 1995). Two dominant double-cleavage ions observed at *m/z* 839.4 and 635.3 represented the structures $[(Me\text{-}Hex)_2(Hex)_2\text{-}28 + Na]^+$ and $[(Me\text{-}Hex)_2(Hex)\text{-}28 + Na]^+$, respectively, indicating two branching points within a sequence of hexoses. The double glycosidic cleavage ions suggested two topologies. One glycan structure carried a branched hexose side chain containing three hexoses (see Figure 4a); the other species contained two hexose residues in the side chain and a third hexose attached to the middle mannose of the GPI anchor glycan core (see Figure 4b). A minor disaccharide fragment ion at *m/z* 431.2 $[Me(Hex)_2\text{-}14 + Na]^+$ further supported these topologies. In contrast, an internal fragment ion at *m/z* 621.35 $[(Hex)_3\text{-}14 + Na]^+$ defined only one branching point in a sequence of four hexoses, suggesting a linear side chain of three alpha-galactose residues attached to the third mannose of the GPI anchor core (see Figure 4c).

Fragments that help define 1→6, 1→4 and 1→2 linkages are derived from double-cleavage across the pyranose ring (Reinhold et al. 1995). Cross-ring cleavage ions at *m/z* 505.2, 533.2, 723.3 and 1349.5 could be identified, though they were relatively weak (see Figure 4, indicated with black arrows). The *m/z* 533.2 and *m/z* 505.2 ions, which were 88 and 60 amu above the glycosidic fragment ion at *m/z* 445.2, $[Me(Hex)_2 + Na]^+$, indicated the Hex_2 moiety to be 6-linked (see Figure 5a). Thus, this ion is consistent with a 1→6 linkage in the trimannosyl GPI core (i.e., Man-Man1-6Man) and in the linear trigalactosyl side chain (i.e., Gal-Gal1-6Gal). The cross-ring fragment ion observed at *m/z* 1349.5 defined the trimannosyl core to be linked to the 4-position of the glucosamine, as it resided 88 amu above the B-type ion at *m/z* 1261.5, and a 60-amu increment could not be detected (see Figures 4 and 5b). This arrangement was further supported by an ambiguous A-type ion at *m/z* 723.3, which was 74 amu above the ion at *m/z* 635.3, $[Me(Hex)_3\text{-}14 + Na]^+$ (see Figure 5c). Together, these results were consistent with the presence of the conserved sequence Manα1-2Manα1-6Manα1-4GlcN, present in almost all GPI anchor structures characterized so far (Ferguson et al. 2008).

Sequence, branching and linkage assignments for the Gal_4 GPI glycan glycoforms

The tandem mass spectrum for the *m/z* 973.9 ion provided an analogous series of monosodium adducts to those recorded in the spectrum of the Gal_3-glycoform (Figure 6, see spectrum). The branching was revealed by double-cleavage ions at *m/z* 635.3, 825.3 and 839.4. The D-type ion observed at *m/z* 635.3 represents the structure $[Me(Hex)_3\text{-}14 + Na]^+$, indicating one branching point in a linear sequence of three hexoses, as described in Ferguson et al. (1988) (Figure 6a). In addition, the ion at *m/z* 825.3 $[Me(Hex)_4\text{-}28 + Na]^+$ supports the topology of two branching points within a sequence of four hexoses (Figure 6b). Evidence for an additional hexose attached to the middle mannose of the GPI anchor was provided by the ion at *m/z* 839.4 $[(Me\text{-}Hex)_2(Hex)_2\text{-}28 + Na]^+$ (Figure 6c). This ambiguous double-cleavage ion could also indicate the presence of a branched three-hexose side chain (Figure 6c). An

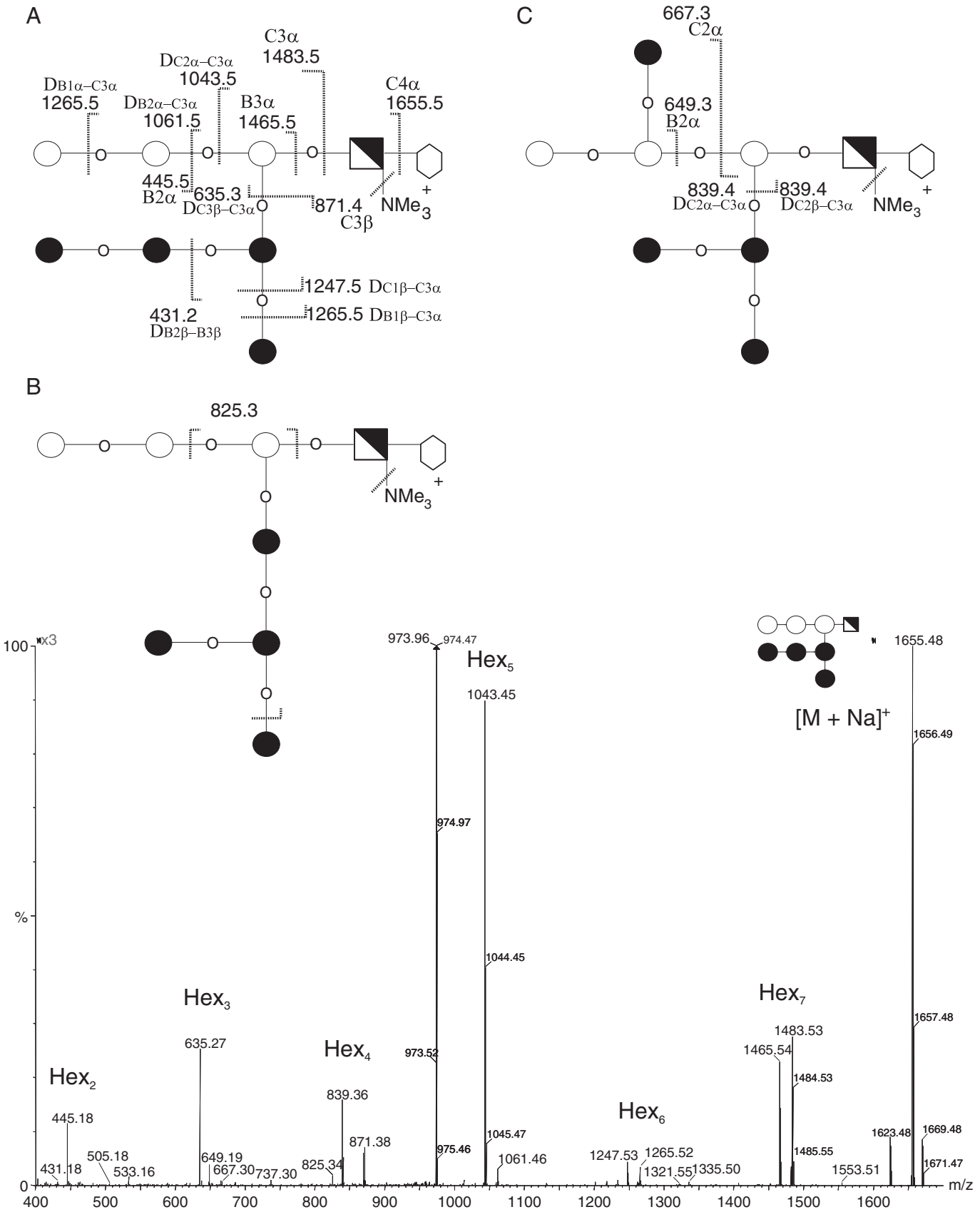

Fig. 6. Product ion spectrum of the permethylated Gal_4-glycoform of the $[M + Na]^{2+}$ precursor ion (*m/z* 973.9). For further discussion, see text.

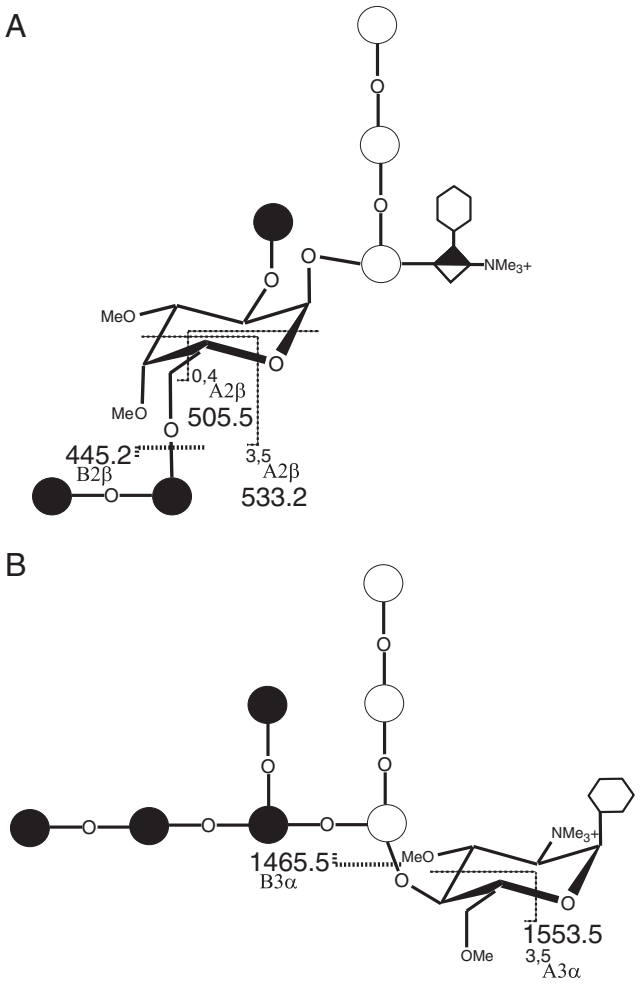

Fig. 7. Cross-ring fragmentation of the permethylated GPI Gal_4-glycoform of the doubly charged precursor ion at *m/z* 973.9. For further discussion, see text.

arrangement of three linear hexose residues in the side chain was supported by the occurrence of a single glycosidic cleavage ion at *m/z* 649.2 $[Me(Hex)_3 + Na]^+$ (not drawn). A linear side chain consisting of four hexose residues was indicated by the ambiguous ion at *m/z* 635.3 $[Hex_4 + Na]^+$ (internal cleavage fragment, not drawn).

Cross-ring fragment ions were also present in the spectrum of the sVSG121 GPI anchor Gal_4-isoform (Figure 6). The ions at *m/z* 533.2 and 505.2 are consistent with the 1→6 linkage between the middle mannose and the mannose next to the glucosamine of the GPI anchor core, as shown for the Gal_3-isoform (see Figure 4a). However, the same ions could also originate from within the branched Gal side chain (see Figure 7a). The A-type ion identified at *m/z* 1553.5, which derived from the double-cleavage ion at *m/z* 1465.5 $[Me(Hex)_7, Na]^+$, permitted the assignment of a 1→4 linkage between the third mannose and the glucosamine (Figure 7b).

Sequence, branching and linkage assignments for the Gal_5 GPI glycan glycoforms

The CID spectrum of the Gal_5-isoform showed similar features to the corresponding Gal_3- and Gal_4-glycoforms (see Figure 8). Glycosidic cleavages resulting in the successive loss of hexose residues dominated the spectrum. Due to the ambiguity of many glycosidic fragment ions derived from this glycan, many different branching topologies are possible. Figure 8 also shows a structure of the Gal_5-glycoform, which corresponds to the known sequence of the sVSG117 Gal_5-glycoform (Mehlert et al. 1998). This structure was supported by the double-cleavage ion observed at *m/z* 839.4 $[(Me\text{-}Hex)_2(Hex)_2\text{-}28 + Na]^+$, indicating an additional hexose attached to the middle mannose of the GPI anchor core. The presence of glycosidic cleavage ions at *m/z* 871.4 (C-type ion) and 853.5 (B-type ion) confirmed the structural feature of a side chain consisting of four hexose residues. However, no ion was detected that could describe a branching point within the side chain unambiguously. Cross-ring fragments were less abundant and had lower intensities when compared to the CID spectra of the Gal_3- and Gal_4-glycoforms. Due to their very weak signals, they were not analyzed further.

GC-MS methylation linkage analysis of sVSG121 GPI glycoforms

In order to confirm the types of linkages assigned for the Gal_3- and Gal_4-glycoforms, a GC-MS methylation linkage analysis was performed using the sVSG121 glycan mixture. The permethylated glycans were hydrolysed, reduced and acetylated to form partially methylated alditol acetates (PMAAs), as described in Ferguson (1994). The PMAAs were resolved by GC-MS (Agilent). The chromatogram (not shown) revealed the presence of a minimum of one terminal mannose, one terminal galactose, one 2-*O*-substituted mannose, one 2-*O*-substituted galactose, one 6-substituted galactose, one 2,3-disubstituted mannose, one 3,6-disubstituted mannose and one 2,6-disubstituted galactose. Figure 9 shows the largest of the structures of the sVSG121 neutral glycans consistent with their GC-MS analysis and previous analyses of GPI anchors from other VSG variants (Ferguson et al. 1988; Mehlert et al. 1998). Sequence, branching and linkage types were consistent with the proposed structures of ions found by CID-MS. Since cross-ring rupture ions of permethylated glycans cannot provide structural information of 1→3 linkages (Reinhold et al. 1995), 3-substituted hexoses could not be detected by CID-MS. Cross-ring cleavage fragments of terminal hexoses were also absent in the CID-MS spectra, possibly due to the very weak signal of the $[Me\text{-}Hex + Na]^+$- precursor ions. The anomeric configurations of the sugar residue that are given in Figure 9 are taken from the fully characterized sVSG221 GPI anchor (Mehlert et al. 1998) and cannot be determined by either GC-MS or CID-MS.

Discussion

Here, we describe the use of soft ionization electrospray mass spectrometry as a powerful technique for structural characterization of glycosylphosphatidylinositol membrane anchors from low picomole amounts of material. We show that sequence, branching and some linkage details of GPI glycans can be deduced from ES-MS/MS data and that these assignments are consistent with previous research on structural characterization of GPI anchors from *T. brucei* (Ferguson et al. 1988; Mehlert et al. 1998). Our method involved the per-

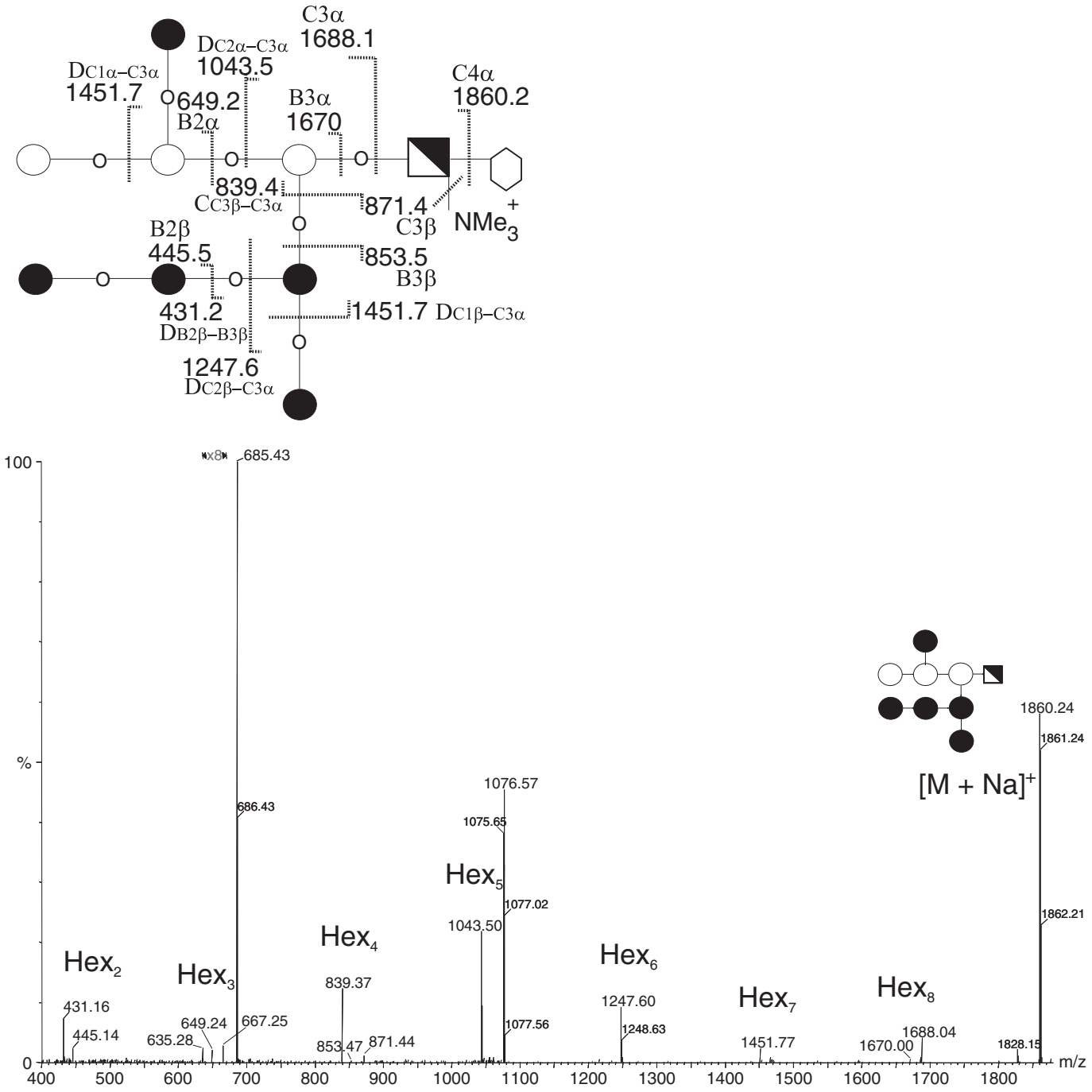

Fig. 8. Product ion spectrum of the permethylated GPI Gal_5-glycoform of the $[M + Na]^{2+}$ precursor ion (*m/z* 1076). For further discussion, see text.

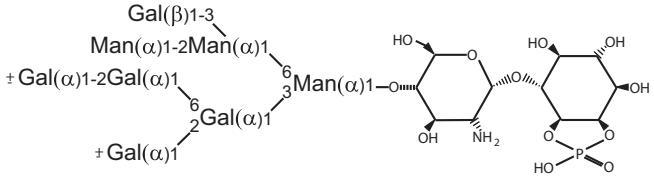

Fig. 9. Proposed structure of sVSG121 neutral glycan as analyzed by GC-MS. The highly conserved core of GPI anchors shows a variety of linear and branched galactosyl substituents specific to *T. brucei*.

methylation of GPI membrane anchor glycans, which is the most important type of derivatization used in oligosaccharide MS (North et al. 2009) followed by positive ion ES-MS and CID-MS. The ES-MS data alone revealed the composition of three different galactose glycoforms of the sVSG121 variant GPI glycan structure (Gal_3–Gal_5), which ionized as doubly charged sodium adducts $[M + Na]^{2+}$. Collision-induced dissociation provided sequences information by producing characteristic glycosidic cleavage ions. Taking into account the conserved Manα1-2Manα1-6Manα1-4GlcN motif found

in almost all GPI structures (Fankhauser et al. 1993), the sequence information could be refined and fitted to a model of a core sequence of Man–Man–Man–GlcN–Ino substituted with Gal residues. Sequence information regarding the branching pattern of the GPI anchor galactose residues around the mannose core of the different glycoforms could also be obtained by ES-MS/MS. Double glycosidic cleavage ions revealed the presence of branched and linear galactose side chains from one up to five residues. However, due to the ambiguity of some glycosidic fragment ions, especially when analyzing more complex glycan structures (e.g. Gal_5-glycoform of sVSG121), complementary analytical methods have to be taken into consideration. The data also provided an indication of hexose linkage composition by observing cross-ring fragment ions of the permethylated GPI glycans, which was consistent with results obtained by GC-MS analysis from the same material. Cross-ring cleavage ions defined the linkage types within the conserved Manα1-2Manα1-6Manα1-4GlcN core, except for terminal hexoses, which is possibly due to the very weak signals of the $[Me\text{-}Hex + Na]^+$- product ions by ES-MS/MS.

Modern ultra-high sensitive mass spectrometry is commonly used for screening samples for specific classes of analytes. In recent years, MS strategies for screening different types of oligosaccharides present in a diverse range of biological materials have been developed to investigate the glycome (North et al. 2009). Often, these methods are based on the analysis of permethylated oligosaccharides and detection of characteristic product ions upon fragmentation. A triple quadrupole mass spectrometer is well suited to screen for the presence of analytes via the use of constant neutral loss and precursor ion scan modes. Unfortunately, sensitive screening for permethylated GPI glycans in complex biological samples using neutral loss scanning is ruled out by the fact that the most abundant reporter ions generated by collision-induced dissociation result from a *non-neutral* loss of the D-*myo*-inositol residue together with the quaternary ammonium ion of the derivatized glucosamine. The principal mass transition for each permethylated GPI glycan is, therefore, from the doubly charged $[M + Na]^{2+}$ precursor ion to singly charged $[(M - 292) + Na]^+$ ion, making the transition different for each value of M. On the other hand, calculated $[M + Na]^{2+}$ to $[(M - 292) + Na]^+$ transitions can be used to build multiple reaction monitoring methods to sensitively search for permethylated GPI glycans of predetermined composition. The scope for precursor ion scanning for permethylated GPIs is also limited by the aforementioned dominant non-neutral loss. Thus, the intensities of all of the other product ions are relatively low (note that in the spectra shown in Figures 4, 6 and 8 the *y*-axis is magnified five, three and eight times, respectively, relative to the 1451.5, 1655.5 and 1859.7 $[(M - 292) + Na]^+$ product ions). Furthermore, product ions that are common to all or most permethylated GPI glycans also tend to be rather nonspecific; for example, the $[Me\text{-}Hex_2 + Na]^+$, $[Hex_3 + Na]^+$ and $[Hex_4 + Na]^+$ product ions at *m/z* 445, 635 and 839, respectively, could also belong to permethylated oligomannose N-linked glycans.

While this study has focused on Q-Tof MS^2 experiments, we are aware that many laboratories now have access to ion trap instruments capable of MS^3 and higher-order experiments. We have only begun to explore the potential of this type of methodology to resolve some of the ambiguities referred to in the MS^2 interpretations herein, but it should, in many cases, resolve alternative branching structures. One such example was recently published by us (Izquierdo et al. 2009), where isolation of $[(M - 292) + 2\ Na]^{2+}$ ions, derived from two isobaric $[M + 2\ Na]^{3+}$ permethylated GPI glycan precursor ions, generated unique and highly informative MS^3 product ion spectra that discriminated two alternative side-chain branching patterns.

Materials and methods

Materials

Sephacryl S200 and QAE-Sephadex A-25 were supplied by Pharmacia, DEAE-cellulose (DE52) by Whatman, Bio-Gel P4 and AG 50W-X12 resin by Bio-Rad, HiTrap SP HP ion exchange column by Amershan Bioscience, 2 ml glass vials, dimethyl sulfoxide and methyl iodide by Sigma-Aldrich and HPTLC plates and Pronase protease from Merck. All other solvents (HPLC grade) were from VWR.

Purification of sVSG121

sVSG MIT_{at}.1.6 (also known as variant 121) was purified from bloodstream form *T. brucei* strain 427 variant MIT_{at}.1.6 cells using hypotonic lysis and DE52 chromatography, as described by Cross (1984). The VSG was further purified by gel filtration using Sephacryl S200 column (4 × 90 cm) equilibrated with 0.1 M NH_4HCO_3. Typically, 10 mg freeze-dried sVSG was obtained from 10^{10} cells.

Preparation of the sVSG MIT_{at}.1.6 GPI neutral glycans

Approximately 1 mg of sVSG121 was treated with 50 µl 50% aqueous HF (48 h at 0°C), freeze-dried (Micro Modulyo), resuspended in 50 µl water and sonicated for 15 min (Ultrasonics Ltd.). The insoluble material was removed by centrifugation (15,000 rpm, 5 min) and washed twice with 20 µl water. The combined supernatants were transferred into a 2-ml glass vial and dried in a Speedvac concentrator (Stratech Scientific). After addition of 50 µl methanol and drying, the GPI glycans were used for permethylation.

GPI glycan permethylation

The GPI glycans were resuspended in 50 µl dimethyl sulfoxide, left for 20 min at room temperature and deprotonated by adding a solution of 120 mg/ml sodium hydroxide in dimethyl sulfoxide (20 min). Methyl iodide was added in three intervals over a total of 30 min (10 µl, 10 min incubation; another 10 µl, 10 min incubation, then 20 µl, 10 min incubation), and the permethylation reaction was continued for another 30 min. The permethylated glycans were partitioned between 250 µl chloroform and 1 ml of 100 mg/ml sodium thiosulphate in water. The upper aqueous phase was removed and the chloroform phase re-extracted six times with 1 ml of water each. The permethylated glycans recovered in the lower chloroform phase were transferred into a new glass vial, dried under N_2 and redissolved in 200 µl of 80% acetonitrile, 0.5 mM sodium acetate for ES-MS analysis.

Electrospray mass spectrometry

Mass spectrometric data was acquired on a Q-Tof2™ (Micromass) hybrid quadrupole time-of-flight instrument. Mass spectra were recorded by linear scanning over a range of *m*/*z* 500–2500. Several scans were summed from a 4 μl introduction of sample solution (100 pmol μl^{-1} of sVSG121 glycan) in 80% acetonitrile containing 0.5 mM sodium acetate using type-F nanotips (Micromass). The data acquired were averaged and processed using the Mass-Lynx software supplied with the instrument. Positive ion spectra were recorded with a tip voltage of 1 kV and a cone voltage of 35–50 V. Fragment ion spectra from the doubly charged pseudomolecular ions were obtained by collision-induced fragmentation in the collision cell using argon as the collision gas at a pressure of 1 bar. The CID mass spectra were recorded by linear scanning over the *m*/*z* range 200–2200. Glu-fibrinopeptide B (Glu-fib) was used as an internal standard for mass calibration at 1 pmol μl^{-1} in 90% acetonitrile containing 0.1% formic acid.

Funding

This work was supported by a Wellcome Trust prize studentship to I.R.E.N., a Medical Research Council program grant to M.A.J.F. and A.M., and a Wellcome Trust Strategic Award [083481] to the Division of Biological Chemistry and Drug Discovery.

Abbreviations

CID, collision-induced dissociation; ER, endoplasmic reticulum; ES, electrospray; GC-MS gas chromatography-mass spectrometry; GPI, glycosylphosphatidylinositol; GPI-AP, glycosylphosphatidylinositol anchored protein; HF hydrogen fluoride; MS, mass spectrometry; MS/MS, tandem mass spectrometry; PMAAs, partially methylated alditol acetates; sVSG, soluble variant surface glycoprotein; *T. brucei*, *Trypanosoma brucei*.

References

Baldwyn MA. 2005. Analysis of glycosylphosphatidylinositol protein anchors: the prion protein. *Method Enzymol.* 405:172–187.

Cross GAM. 1984. Release and purification of Trypanosoma brucei variant surface glycoprotein. *J Cell Biochem.* 24:79–90.

Domon B, Costello C. 1988. A systematic nomenclature for carbohydrate fragmentation in FAB-MS/MS spectra of glycoconjugates. *Glycoconjugate J.* 5:397–409.

Fankhauser C, Homans SW, Thomas-Oates JE, McConville MJ, Desponds C, Conzelmann A, Ferguson MAJ. 1993. Structures of glycosyl-phosphatidylinositol membrane anchors from *Saccharomyces cerevisiae*. *J Biol Chem.* 268:26365–26374.

Ferguson MAJ. 1994. GPI membrane anchors: isolation and analysis. In: Fukuda M and Kobata A, editors. *Glycobiology: A Practical Approach*. Oxford: IRL Oxford Univ. Press. p. 349–383.

Ferguson MAJ, Homans SW, Dwek RA, Rademacher TW. 1988. Glycosylphosphatidylinositol moiety that anchors *Trypanosoma brucei* variant surface glycoprotein to the membrane. *Science.* 239:753–759.

Ferguson MAJ, Kinoshita T, Hart GW. 2008. Glycosylphosphatidylinositol membrane anchors. In: Varki A, Cummings RD, Esko JD, Freeze HH, Stanley P, Bertozzi CR, Hart GW and Etzler ME, editors. *Essential Glycobiology.* Second Edition, New York: Cold Spring Harbor Laboratory Press. p. 143–162.

Fujita M, Kinoshita T. 2010. Structural remodeling of GPI anchors during biosynthesis and after attachment to proteins. *FEBS Lett.* in press.

Homans SW, Ferguson MAJ, Dwek RA, Rademacher TW, Anand R, Williams AF. 1988. Complete structure of the glycosyl phosphatidylinositol membrane anchor of rat brain Thy-1 glycoprotein. *Nature.* 333:269–272.

Izquierdo L, Nakanishi M, Mehlert A, Machray G, Barton GJ, Ferguson MAJ. 2009. Identification of a GPI-anchor modifying β1-3 *N*-acetylglucosaminyltransferase in *Trypanosoma brucei*. *Mol Microbiol.* 71:478–491.

Mehlert A, Richardson JM, Ferguson MA. 1997. The core glycosylphosphatidylinositol anchor structures of *Trypanosoma brucei* variant surface glycoprotein 221. *Biochem Soc Trans.* 25:13S.

Mehlert A, Richardson JM, Ferguson MAJ. 1998. Structure of the glycosylphosphatidylinositol membrane anchor glycan of a class-2 variant surface glycoprotein from *Trypanosoma brucei*. *J Mol Biol.* 277:379–392.

Moody-Haupt S, Patterson JH, Mirelman D, McConville MJ. 2000. The major surface antigens of *Entamoeba histolytica* trophozoites are GPI-anchored proteophosphoglycans. *J Mol Biol.* 297:409–420.

North SJ, Hitchen PG, Haslam SM, Dell A. 2009. Mass spectrometry in the analysis of N-linked and O-linked glycans. *Curr Opin Struct Biol.* 19:498–506.

Paulick MG, Bertozzi CR. 2008. The glycosylphosphatidylinositol anchor: a complex membrane-anchoring structure for proteins. *Biochemistry.* 47:6991–7000.

Reinhold VN, Reinhold BB, Costello CE. 1995. Carbohydrate molecular weight profiling, sequence, linkage, and branching data: ES-MS and CID. *Anal Chem.* 67:p. 1772–1784.

Schneider P, Ferguson MAJ, McConville MJ, Mehlert A, Homans SW, Bordier C. 1990. Structure of the glycosyl-phosphatidylinositol membrane anchor of *Leishmania major* promastigote surface protease. *J Biol Chem.* 265:16955–16964.

Strang AM, Allen AK, Holder AA, van Halbeek H. 1993. The carbohydrate structures of *Trypanosoma brucei brucei* MITat 1.6 variant surface glycoprotein. A re-investigation of the C-terminal glycan. *Biochem Biophys Res Commun.* 196.

Zitzmann N, Mehlert A, Carrouée S, Rudd PM, Ferguson MA. 2000. Protein structure controls the processing of the N-linked oligosaccharides and glycosylphosphatidylinositol glycans of variant surface glycoproteins expressed in bloodstream form *Trypanosoma brucei*. *Glycobiology.* 10:243–249.